DOI: 10.1002/JLB.4MA0620-526RR

JLB JOURNAL OF LEUKOCYTE BIOLOGY

ARTICLE

Guanylate binding proteins contained in the murine chromosome 3 are important to control mycobacterial infection

Fabio V. Marinho[1] | Julia S. Fahel[1] | Ana Carolina V. S. C. de Araujo[1] | Lunna T. S. Diniz[1] | Marco T. R. Gomes[1] | Danilo P. Resende[2] | Ana P. Junqueira-Kipnis[2] | Sergio C. Oliveira[1]

[1]Department of Biochemistry and Immunology, Institute of Biological Sciences, Federal University of Minas Gerais, Minas Gerais, Belo Horizonte, Brazil

[2]Tropical Institute of Pathology and Public Health, Department of Microbiology, Immunology, Parasitology and Pathology, Federal University of Goias, Goias, Goiania, Brazil

Correspondence
Dr. Sergio Costa Oliveira, Laboratório de Imunologia de Doenças Infecciosas, Departamento de Bioquímica e Imunologia, Universidade Federal de Minas Gerais, Avenida Antônio Carlos 6627, Pampulha, Belo Horizonte, Minas Gerais 31270-901, Brasil.
Email: scozeus1@gmail.com

Abstract

Guanylate binding proteins (GBPs) are important effector molecules of autonomous response induced by proinflammatory stimuli, mainly IFNs. The murine GBPs clustered in chromosome 3 (GBPchr3) contains the majority of human homologous GBPs. Despite intense efforts, mycobacterial-promoted diseases are still a major public health problem. However, the combined importance of GBPchr3 during mycobacterial infection has been overlooked. This study addresses the influence of the GBPchr3 in host immunity against mycobacterial infection to elucidate the relationship between cell-intrinsic immunity and triggering of an efficient anti-mycobacterial immune response. Here we show that all GBPchr3 are up-regulated in lungs of mice during *Mycobacterium bovis* BCG infection, resembling tissue expression of IFN-γ. Mice deficient in GBPchr3 (GBPchr3$^{-/-}$) were more susceptible to infection, displaying diminished expression of autophagy-related genes (*LC3B*, *ULK1*, and *ATG5*) in lungs. Additionally, there was reduced proinflammatory cytokine production complementary to diminished numbers of myeloid cells in spleens of GBPchr3$^{-/-}$. Higher bacterial burden in GBPchr3$^{-/-}$ animals correlated with increased number of tissue granulomas. Furthermore, absence of GBPchr3 hampered activation and production of TNF-α and IL-12 by dendritic cells. Concerning macrophages, lack of GBPs impaired their antimicrobial function, diminishing autophagy induction and intracellular killing efficiency. In contrast, single GBP2 deficiency did not contribute to in vivo bacterial control. In conclusion, this study shows that GBPchr3 are important not only to stimulate cell-intrinsic immunity but also for inducing an efficient immune response to control mycobacterial infection in vivo.

KEYWORDS
dendritic cells, GBPchr3, macrophages, *Mycobacterium bovis* BCG

1 | INTRODUCTION

Innate immunity is paramount as frontline defense against pathogens or disturbances in cellular homeostasis. Cell-intrinsic mechanisms, also referred to as cell-autonomous immunity, comprise the ability of a cell to sense and to respond injuries in the host cytosol by itself.[1] This kind of immune response is important for myeloid cells to restrain pathogens that survive in membrane-bound compartments, the pathogen-containing vacuoles (PCVs).[1] Among the effector molecules responsible for this innate response are the guanylate binding proteins (GBPs). GBPs comprise a family of interspecies conserved dynamin-like GTPases of 65–73 kDa (small GTPases).[1,2] The human

Abbreviation: BMDC, Bone marrow-derived dendritic cells; BMDM, Bone marrow-derived macrophages; d.p.i., Days post infection; DCs, Dendritic cells; GBP, Guanylate binding proteins; GBPchr3, GBPs from murine chromosome 3 (GBP1, GBP2, GBP3, GBP5 and GBP7); MOI, Multiplicity of infection; PAMP, Pathogen-associated molecular pattern; PCV, Pathogen-containing vacuole; TB, Tuberculosis.

Received: 8 January 2020 | Revised: 1 June 2020 | Accepted: 21 June 2020

GBPs are located in a single cluster on chromosome 1. On the other hand, murine GBPs are divided in two clusters: one on chromosome 3 (now on referred as GBPchr3) that contains the genes for GBP1, GBP2, GBP3, GBP5, GBP7, and one pseudogene, and another on chromosome 5 (GBP4, GBP6, GBP8, GBP9, GBP10, GBP11, and the second pseudogene).[3,4] These proteins are highly induced by IFNs (both type I and type II), although other proinflammatory stimuli, such as TNF-α and TLRs signaling, are also able to induce their expression.[2] The GBPchr3 contains the majority of the human homologous GBPs.[3] These molecules are mainly localized in the cytosol, and some interact with membrane-bound compartments.[5] Upon activation, GBPs can be recruited to the PCVs or the pathogen's membrane and afterward mobilize other GBPs and molecules, contributing to the elimination of the microorganism or to the release of pathogens-associated molecular pattern (PAMPs) that will further activate the cell.[6] The relevance of GBPs in cell-intrinsic immunity against diverse intracellular pathogens among viruses, protozoa, and bacteria is documented (reviewed in Praefcke[7]). For instance, most of the recent studies focused in Gram-negative bacteria and there is a crescent body of evidence concerning GBPs relationship with the caspase-11 noncanonic inflammasome activation.[8,9] Despite that, the influence of GBPs in other aspects of the immune response needs further investigation.

Mycobacteria represent one of the most successful intracellular pathogens. The prototype bacteria of this genus, *Mycobacterium tuberculosis*, causes tuberculosis (TB) and kills about 1.4 million people worldwide annually.[10] Other prominent pathogenic mycobacteria are *Mycobacterium leprae* and *Mycobacterium bovis*, from which *M. bovis* BCG strains were derived, a useful laboratorial replacement to study mycobacteria host-pathogen interactions and the only available vaccine to TB.[11] A major virulence feature of mycobacteria is their ability to block phagosome maturation, to reside and to replicate inside these compartments. The mycobacterial endosome is adapted to sustain this pathogen, retaining the interaction with host endosomal network for accessing essential nutrients such as iron and fats while preventing fusion with lysosomes.[12-15] Among the key mediators of immunity to *M. tuberculosis* and other mycobacteria are TNF-α and IFN-γ,[16-19] both of which are able to activate phagocytes to overcome the blockade and improve killing of the bacilli.[20,21] Their importance is manifested by the reactivation of latent TB during TNF-α therapeutic neutralization or the lethal mycobacteriosis caused by BCG vaccine in patients' deficient for molecules of the IL12/IFN-γ axis.[22,23]

There is limited literature concerning the role of IFN-inducible GTPases superfamily in immunity against mycobacterial infections.[24-26] GBPs are among the most abundantly expressed IFN-stimulated genes.[27] GBP1 and GBP7 are able to limit *M. bovis* BCG growth by recruiting phagocyte oxidase and autophagy effectors to the PCVs inside macrophages.[28] However, the role of GBPs in other aspects of immunity aside from autonomous response is being overlooked so far. Indeed, the combined importance of chromosome 3-encoded GBPs during mycobacterial infection in vivo was not addressed.

This work highlights the cell-intrinsic immunity dependent on GBPchr3 influencing immune response against *M. bovis* BCG infection. Herein, we show that all GBPchr3 are up-regulated in lungs of mice during *M. bovis* BCG infection, in response to IFN-γ expression in this tissue. Moreover, mice deficient for the entire locus of GBPchr3$^{-/-}$ are more susceptible to *M. bovis* BCG infection due to impaired establishment of immune response and have decreased function of myeloid cells.

2 | MATERIALS AND METHODS

2.1 | Animals

C57BL/6 wild-type mice were obtained from the Federal University of Minas Gerais (UFMG) animal facility. GBPchr3$^{-/-}$ and GBP2$^{-/-}$ mice were provided by Dr. Petr Broz (University of Lausanne, Lausanne, Switzerland). All mice were housed in a specific pathogen-free laboratory facility. Female mice were used at 8–10 wk of age. Experiments were performed according to protocols that were approved by the Animal Studies Committee (protocol CEUA 167/2018).

2.2 | Bacteria and growth conditions

Mycobacterium bovis BCG strain Moreau was grown in Middlebrook 7H9 broth that contained 0.05% Tween 80 and 0.2% glycerol and was supplemented with 10% albumin-dextrose-catalase. Cultures were harvested by centrifugation at the mid-exponential phase, suspended in saline containing 0.05% Tween 80, and stored at −80°C until use.

2.3 | In vivo infection and measurement of bacterial burden

Mice ($n = 10$ per group) were infected i.v. with 1×10^6 CFUs of *M. bovis* BCG Moreau after anesthesia with 5% ketamine, 2% xylazine, and 0.9% NaCl. The bacterial load in the spleens, livers, and lungs were determined at 30 and 60 d postinfection (d.p.i.). Briefly, the organs were collected aseptically and homogenized in distilled water that contained 0.05% Tween 80. Serial dilutions of the resulting suspensions were plated in Middlebrook 7H11 agar medium that was supplemented with 10% oleic acid-albumin-dextrose-catalase, and the CFUs were counted after 3–4 wk of incubation at 37°C.

2.4 | Quantitative real-time PCR

Lungs were collected and homogenized in TRIzol reagent (Invitrogen, Carlsbad, CA, USA) to isolate total RNA accordingly to manufacturer instructions. Alternatively, bone marrow-derived macrophages (BMDMs) were stimulated in 24-well plates and homogenized in TRIzol reagent (Invitrogen). Reverse transcription of 2 μg of total RNA was performed in a final volume of 20 μL containing oligo-dT (0.5 μg/μL), dNTP 10 mM, DTT 0.1 M, buffer 5× and reverse-transcriptase (2 U per reaction), using the following cycling parameters: 42°C for 60 min and 70°C for 15 min. Quantitative real-time PCR was conducted in a final volume of 10 μL containing the following: SYBR Green PCR Master Mix

TABLE 1 Primers used for quantitative real-time PCR in this study*

Primer	Forward (5′-3′)	Reverse (5′-3′)
GBP1	GAGTACTCTCTGGAA	TAGATGAAGGTGCTG
	ATGGCCTCAGAAA	CTGAGGAGGACTG
GBP2	CTGCACTATGTGACGGAGCTA	CGGAATCGTCTACCCCACTC
GBP3	CTGACAGTAAATCTGGAAGCCAT	CCGTCCTGCAAGACGATTCA
GBP5	CTGAACTCAGATTTTGTGCAGGA	CATCGACATAAGTCAGCACCAG
GBP7	TCCTGTGTGCCTAGTGGAAAA	CAAGCGGTTCATCAAGTAGGAT
IFNγ	ACAATGAACGCTACACACTGCAT	TGGCAGTAACAGCCAGAAACA
IFNβ	AGCTCCAAGAAAGGACGAACAT	GCCCTGTAGGTGAGGTTGATCT
LC3B	ACTGCTCTGTCTTGTGTAGGTT	TCGTTGTGTGCCTTTATTAGTGCATC
ULK1	CACAGAACGACCAATGGATG	GGTGAAGAGGACAGCTCTGG
ATG5	GATGGACAGCTGCACACACT	TTGGCTCTATCCCGTGAATC
18S	CGTTCCACCAACTAAGAACG	CTCAACACGGGAAACCTCAC
β-actin	AGTGTGACGTTGACATCCGT	TGCTAGGAGCCAGAGCAGTA

*All primer pairs were designed to amplify a specific region of the target murine genes.

(Thermo Fischer Scientific, Waltham, MS, USA), oligo-dT cDNA as the PCR template, and 5 μM of primers. The PCR reaction was performed with QuantStudio 3 Real-Time PCR System (Thermo Fischer Scientific) using the following cycling parameters: 60°C for 10 min, 95°C for 10 min, 40 cycles of 95°C for 15 s, and 60°C for 1 min, and a dissociation stage of 95°C for 15 s, 60°C for 1 min, 95°C for 15 s, and 60°C for 15 s. Primers were used to amplify a specific fragment corresponding to the gene target as shown in Table 1. Data were analyzed using the threshold cycle ($\Delta\Delta C_t$) method and they were presented as relative expression units after normalization to the house keeping gene. PCR measurements were conducted in triplicate.

2.5 | Bronchoalveolar lavage

The tracheas of mice were cannulated and the airway lumen was washed twice with 500 μL of PBS. The recovered fluids were centrifuged 10 min 300 $\times g$ and the supernatant was used for determination of TNF-α and IL-12 levels by ELISA using a DuoSet kit (R&D Systems, Minneapolis, MN, USA), according to the manufacturer's instructions.

2.6 | Spleen cells culture

Cells that were obtained from the spleens of infected mice were washed with saline and the erythrocytes were lysed with a hemolytic solution (155 mM NH4Cl, 10 mM KHCO3, pH 7.2). Spleen cells were seeded at 1×10^6/well into 96-well plates with RPMI 1640 (Gibco, Carlsbad, CA, USA) that was supplemented with 2 mM L-glutamine, 25 mM HEPES, 10% heat-inactivated FBS (Gibco), penicillin G sodium (100 U/mL), and streptomycin sulfate (100 μg/mL). The cells were stimulated with *M. bovis* BCG Moreau (multiplicity of infection [MOI] 5:1). Unstimulated cells were used as negative controls, and cells stimulated with ultra-pure *Escherichia coli* LPS (1 μg/mL; Sigma-Aldrich, St. Louis, MO, USA) or concanavalin A (5 μg/mL; Sigma-Aldrich) were used as positive controls. After 48 or 72 h, TNF-α or IFN-γ production were measured in the cells supernatants by ELISA using a DuoSet kit (R&D Systems), according to the manufacturer's instructions.

2.7 | Flow cytometry analysis

Spleen cells from mice were harvested as mentioned previously and adjusted to 1×10^6 cells/well. Diverse staining panels were used for evaluation of myeloid cells number, level of activation, and cytokine production. Alternatively, a specific staining panel was used for lymphocyte analysis. For cytokine staining, cells were incubated with Brefeldin A (1 μg/well; Sigma-Aldrich) during 4 h at 37°C, 5% CO_2. Briefly, cells were incubated for 20 min with anti-mouse CD16/32 to block Fc receptors (BD Bioscience, Franklin Lakes, NJ, USA) in FACS buffer (PBS, 0.25% BSA, 1 mM NaN3) and were stained for surface markers. For intracellular staining, cells were fixed and permeabilized using BD Cytofix/Cytoperm Kit (BD Biosciences), according to the manufacturer's instructions. The following conjugated antibodies were used: FITC anti-mouse CD11c (clone HL3, BD Bioscience), FITC anti-mouse CD8 (clone 53–6.7, BD Bioscience), PE anti-mouse CD11c (clone HL3; BD Biosciences), PE anti-mouse CD40 (clone 3/23; BD Biosciences), biotin-conjugated anti-mouse F4/80 (clone BM8, eBioscience, San Diego, CA, USA), biotin-conjugated anti-mouse CD8 (clone 53–6.7, BD Biosciences), biotin-conjugated anti-mouse CD3e (clone 500A2, BD Bioscience), PE-Cy7 anti-mouse TNF (clone MP6-XT22; BD Biosciences), allophycocyanin (APC) anti-mouse MHC-II (clone AF6-120.1, BD Bioscience), APC anti-mouse IL-12p70 (clone C15.6, BD Bioscience), APC-Cy7 anti-mouse CD11b (clone M1/70, BD Bioscience), or APC-Cy7 anti-mouse CD4 (clone GK1.5, BD Bioscience). Streptavidin PE-Cy5.5 (Thermo Fisher Scientific) was added where necessary. The appropriate isotype controls were used. Attune Acoustic Focusing Cytometer (Life Technologies, Carlsbad, CA, USA) was used to collect 100,000 events and data were analyzed using FlowJo Software (Tree Star, Ashland, OR, USA). Gating

strategy is shown in Supporting Information Figure S1. Representative 2D-plots of each analysis are also shown together with summary graph. Alternatively, bone marrow-derived dendritic cells (BMDCs) were also evaluated. BMDCs were stained for CD11c, CD11b, and CD40. The protocol used was similar to aforementioned. The appropriate isotype controls were used. Attune Acoustic Focusing Cytometer (Life Technologies) was used to collect around 50,000 events, and data were analyzed using FlowJo Software (Tree Star). Total cells were selected after gating on $CD11b^+CD11c^+$ double positive cells; finally, $CD40^+$ cells were analyzed. The mean fluorescence intensity of CD40 expression was evaluated inside the entire $CD11b^+CD11c^+$ double positive cell population.

2.8 | Histopathology

The left lung and the left lobe of the liver were collected, fixed in 10% buffered formaldehyde solution, dehydrated, diaphanized, and embedded in paraffin. Tissue sections (2–3 μm) were stained with H&E. Digital images of the slides were assessed and captured with an Olympus SC30 camera (Olympus, Tokyo, Japan) using 10× objective lens. The counting of granulomas was performed by identifying the characteristic round-shape inflammatory cells infiltrate in the tissue parenchyma. The total area of each section was measured using ImageJ software (National Institutes of Health, Bethesda, MD, USA; available at http://imagej.nih.gov/ij/), by converting pixels in square millimeters. The results are expressed in granuloma numbers per square millimeter of tissue.

2.9 | Generation of BMDMs or BMDCs and cytokine analysis

Macrophages and dendritic cells (DCs) were derived from the bone marrow of mice. To obtain macrophages, bone marrow cells were removed from the femurs and tibias of the animals and cultured in DMEM (Gibco) with 10% FBS, 1% HEPES, penicillin G sodium (100 U/mL), streptomycin sulfate (100 μg/mL), and 20% L929 cell-conditioned medium in petri dishes (1×10^7 cells). The cells were cultured at 37°C in an atmosphere of 5% CO_2. After 4 d, 10 mL of fresh medium was added. At day 7 in culture, the cells had completely differentiated into macrophages. To obtain DCs, bone marrow cells were cultured in RPMI 1640 with 10% FBS, penicillin G sodium (100 U/mL), streptomycin sulfate (100 μg/mL), and 20 ng/mL murine recombinant granulocyte-M-CSF (GM-CSF; Peprotech, Ribeirão Preto, SP, Brazil) in petri dishes (1×10^7 cells). The cells were cultured at 37°C in an atmosphere of 5% CO_2. At day 3 of incubation, a further 5 mL of fresh complete medium with GM-CSF were added, and an additional 5 mL of fresh medium containing GM-CSF was replaced on days 5 and 7. At day 10, nonadherent cells were harvested. Macrophages and DCs were seeded in 24-well plates (5×10^5 cells) or 96-well plates (1×10^5 cells) and used for in vitro studies. Stimulation of the BMDMs and BMDCs was performed by the addition of supplemented DMEM with *M. bovis* BCG Moreau (MOI 5:1) or ultra-pure *E. coli* LPS (100 ng/mL, Sigma-Aldrich). Culture supernatants were collected after 24 h of stimulation and subsequently used for cytokine and cytometry analysis. For RNA expression measurement, the cells were stimulated with *M. bovis* BCG (MOI 5:1) during 18 or 48 h.

2.10 | Western blot

BMDMs (5×10^5 cells/well) were obtained and infected with *M. bovis* BCG Moreau (MOI 50:1) or stimulated with 15 μg/ml of rapamycin in a 24-well plate for 4 h. When determined, Bafilomycin A1 (100 nM; Sigma-Aldrich) was added for the 4 h of stimulation period. After that, cells were washed and lysed using M-PER Mammalian Protein Extraction Reagent (Thermo Fisher Scientific) supplemented with 1 mM sodium orthovanadate, 10 mM NaF and 1:100 of protease inhibitor cocktail (Sigma-Aldrich), and stored at −80°C. Then 15 μg of total protein from each sample were resolved in a 15% SDS-PAGE and the separated proteins were electrotransferred to a nitrocellulose membrane. Endogenous LC3 conjugation was evaluated by Western blot analysis using monoclonal antibodies against LC3B and β-actin (clone 13E5) (both from Cell Signaling Technology, Danvers, MA, USA). The protein bands were visualized using Luminol chemiluminescent HRP substrate (Millipore, Billerica, MA, USA) in an Amersham Imager 600 (GE Healthcare, Buckinghamshire, United Kingdom). Densitometry analysis was performed using ImageJ software.

2.11 | In vitro infection and measurement bacterial intracellular growth

BMDMs (5×10^5 cells/well) were infected with *M. bovis* BCG Moreau (MOI 5:1) in 300 μL/well of DMEM supplemented with 10% FBS and 1% HEPES. Cells were incubated for 4 h at 37°C in a 5% CO2 atmosphere, then washed with warm saline to remove noninternalized bacteria, and reincubated in supplemented DMEM for up to 7 d. To quantify the number of intracellular bacteria, macrophages were lysed immediately (T0), 2 and 7 d.p.i. with 0.1% saponin (Sigma-Aldrich). Serial dilutions were plated in Middlebrook 7H11 agar medium that was supplemented with 10% oleic acid-albumin-dextrose-catalase, and the CFUs were counted after 3–4 wk of incubation at 37°C.

2.12 | Nitrite measurement by Griess reagent

The supernatants of 72 h stimulated spleen cells were used for nitrite measurement. Alternatively, BMDMs (1×10^5 cells/well) were incubated overnight with recombinant murine IFN-γ (10 ng/mL) and then stimulated with *M. bovis* BCG Moreau (MOI 5:1) or ultra-pure *E. coli* LPS (100 ng/mL, Sigma-Aldrich) for 24 h. The concentration of nitrite (NO_2^-), a stable metabolite of NO, was measured using Griess reagent (1% sulfanilamide and 0.1% naphthyl ethylenediamine dihydrochloride in 2.5% phosphoric acid). Briefly, 50 μL of cell culture supernatants were mixed with 50 μL of Griess reagent. Subsequently, the mixture was incubated protected from light at room temperature for 5 min and the absorbance at 550 nm was measured in a microplate reader. Fresh culture medium was used as blank. The quantity of nitrite was determined from a sodium nitrite ($NaNO_2$) standard curve.

2.13 | Statistical analysis

Results are presented as the mean ± SD. Statistically significant differences among the results obtained were evaluated by 2-way ANOVA followed by the Bonferroni post hoc test ($P < 0.05$), 1-way ANOVA followed by the Tukey post hoc test ($P < 0.05$) or the Student *t*-test ($P < 0.05$). Statistical analysis was performed using GraphPad Prism 5.0 (GraphPad Software, San Diego, CA, USA)

3 | RESULTS

3.1 | GBPs from murine chromosome 3 are up-regulated in lungs during *M. bovis* BCG infection

Mycobacteria are pathogens sensitive to IFN-γ-dependent immune responses, a scenario that may involve GBPs. To mimic systemic mycobacterial dissemination, and address the implication of GBPs from mouse chromosome 3 in host defense against *M. bovis* BCG Moreau strain, wild-type animals were infected i.v. and evaluated at 30 and 60 d.p.i for *GBPs* expression in lungs. It was observed that all GBPchr3 (GBPs 1, 2, 3, 5, and 7) were significantly up-regulated during the time points observed, with a remarkable up-regulation during early infection period (30 d.p.i; Fig. 1A). *GBP2*, *GBP3*, and *GBP7* presented similar up-regulation levels whereas GBP5 was highly induced, reaching more than 300 times mRNA expression compared to noninfected animals. *GBP1* was also up-regulated, although with more modest numbers. After 60 d of infection, all GBPs analyzed dropped considerably to a similar level of gene expression. The GBP up-regulation pattern followed the peak of *IFN-γ* expression observed in lungs of infected animals (Fig. 1B). During early infection there was also higher expression of *IFN-β* in lung tissue, although it did not reach compelling levels. Both type I and type II IFNs could be contributing to higher levels of *GBPs* expression observed.

One of the main cell-intrinsic mechanisms to limit intracellular bacteria is the autophagy, a unique lysosomal degradation pathway that is triggered for elimination of cytoplasmic materials.[29] This is a complex process where different effector proteins such as LC3B, ULK1, and ATG5 take place during the autophagosome maturation.[30] In order to evaluate if autophagy induction was related to the up-regulation of GBPs, the expression of *LC3B*, *ULK1*, and *ATG5* genes were addressed during early mycobacterial infection. In this regard, 30 d infected mice deficient for the entire locus of GBPchr3 (GBPchr3$^{-/-}$) were compared to their wild-type counterparts. Figure 1C shows that all these autophagy genes were up-regulated due to infection. Interestingly, lack of GBPchr3 diminished significantly the expression of *LC3B*, *ULK1*, and *ATG5* (Fig. 1C).

In summary, these results demonstrate that during early mycobacterial infection GBPchr3 are up-regulated, concomitant with *IFN-γ* expression. Additionally, high level of expression of autophagy genes requires GBPchr3.

3.2 | Absence of GBPs from murine chromosome 3 renders mice more susceptible to *M. bovis* BCG infection

GBPs are important for cell-intrinsic immunity but their importance during the establishment of innate immune responses during mycobacterial infections have been less investigated. To address the influence of GBPs in vivo, GBPchr3$^{-/-}$ or single deficient for GBP2 (GBP2$^{-/-}$) mice were infected with *M. bovis* BCG and monitored at 30 or 60 d.p.i. The lack of GBPchr3 resulted in high bacterial burden compared to wild-type (WT) mice, especially in liver and lungs (Fig. 2). Surprisingly, absence of GBP2 alone did not alter the bacterial burden of infected mice. To investigate the underlying factors responsible for the increased susceptibility of GBPchr3$^{-/-}$ mice, other immunologic parameters were evaluated focusing on early infection (30 d.p.i.), once highest GBPs expression was observed at this time point. GBPchr3-deficient mice showed lower levels of TNF-α and IL-12 in bronchoalveolar lavage compared to WT animals (Fig. 3A, B). Moreover, absence of GBPchr3 reduced the systemic recall responses of TNF-α and IFN-γ, and production of NO by spleen cells in response to *M. bovis* BCG (Fig. 3C–E). We also observed decreased frequency of macrophages (CD11b$^+$F4/80$^+$ cells) and subpopulations of classic DCs (cDCs) (CD11b$^+$CD11c$^+$ cells—CD11b+ DCs—and CD8$^+$CD11c$^+$ cells—CD8+ DCs) in spleen of knockout mice at 30 d.p.i (Fig. 3F–H). Both cDCs are present in spleen. CD11b+ DCs often predominates and have a prominent role in MHC-II presentation and activation of CD4+ T cells. On the other hand, CD8+ DCs have a superior ability to cross-present antigens.[31] It is worth noticing that the expression of activation markers as well as production of proinflammatory cytokines by these myeloid populations were reduced in GBPchr3$^{-/-}$ mice (Supporting Information Fig. S2). By contrast, there was higher presence of CD4+ T cells in GBPchr3-deficient mice, suggesting a compensatory effect because myeloid cell populations were reduced and inadequately activated (Supporting Information Fig. S3). The higher bacterial burden observed correlated with increased number of granulomas in lungs and liver of GBPchr3$^{-/-}$ mice when compared to WT animals (Fig. 4). Interestingly, there is a mild reduction in TNF-α and IFN-γ recall response in GBPchr3$^{-/-}$ mice retained until late infection (60 d.p.i), although the presence of myeloid cells restored to wild-type levels (Supporting Information Fig. S4). Altogether, these results demonstrate that absence of GBPchr3 compromise the in vivo control of *M. bovis* BCG, influencing the immune response in different sites of infection.

3.3 | Deficiency on the cluster of GBPs from chromosome 3 affects dendritic cells activation

DCs are important Ag-presenting cells that orchestrate the establishment of immune responses. To address whether the GBPchr3 have a role during activation of these cells, BMDCs were stimulated for 24 h with *M. bovis* BCG. Interestingly, the production of proinflammatory cytokines TNF-α and IL-12 was diminished in GBPchr3$^{-/-}$

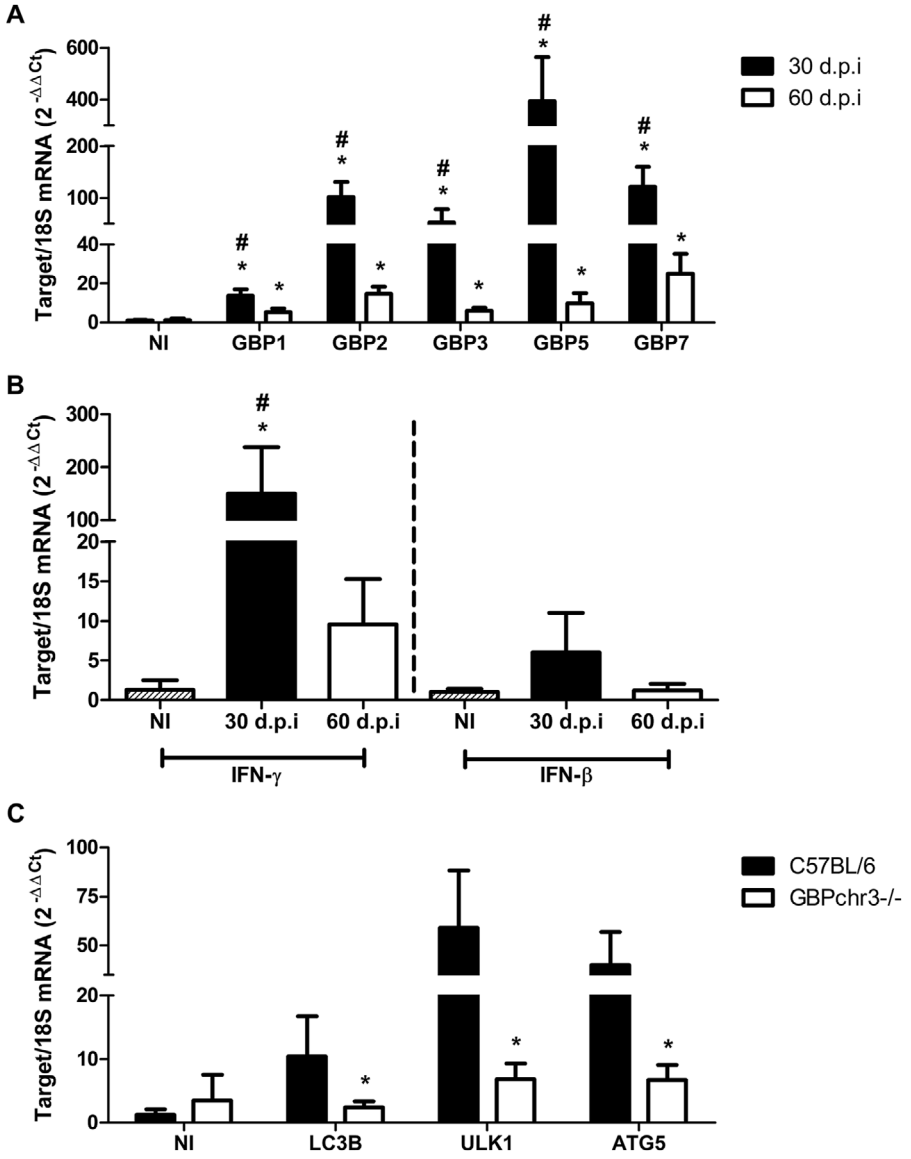

FIGURE 1 **The guanylate binding proteins (GBPs) from chromosome 3 (GBPchr3) are highly expressed in lungs during early infection by *Mycobacterium bovis* BCG.** The lungs from 30 or 60 d infected C57BL/6 mice were collected for RNA extraction. (**A**) *GBPs* or (**B**) *IFN-γ* and *IFN-β* expression levels were evaluated by qPCR and normalized to noninfected samples. (**C**) The expression level of the autophagy-related genes *LC3B*, *ULK1*, and *ATG5* were analyzed in lungs from 30 d infected C57BL/6 and GBPchr3$^{-/-}$ mice. All results were relative to 18S mRNA. NI: noninfected; $^{*}P < 0.05$ compared to NI; and $\#P < 0.05$ compared to 60 d.p.i

compared to wild-type DCs (Fig. 5A, B). Additionally, the expression of CD40, an important costimulatory molecule for activation of adaptive immune response, was significantly reduced in deficient cells (Fig. 5C, E; Supporting Information Fig. S5A). These results suggest that GBPchr3 participate in the activation of DCs in response to *M. bovis* BCG infection.

3.4 | Lack of GBPs from chromosome 3 hampers macrophages function against *M. bovis* BCG

Macrophages are the main cells that harbor mycobacteria during infection. These cells are the focus of observation concerning GBP-mediated autonomous responses. Indeed, infection with *M. bovis* BCG is sufficient to induce the expression of GBPchr3 in wild-type BMDMs (Fig. 6A). In order to investigate further the importance of the cluster of GBPchr3 in macrophage function, BMDMs from GBPchr3$^{-/-}$ mice were infected and several parameters analyzed. First, the production of TNF-α and NO was reduced due to lack of GBPchr3 (Fig. 6B, C).

LC3 is a crucial autophagic marker. It can be found in two configurations inside the cell: LC3-I, the cytosolic form, and LC3-II, the lipidated and autophagosome-associated form. LC3-I to LC3-II conversion is commonly used to access autophagosome formation.[32] In this regard, autophagy induction in response to *M. bovis* BCG infection was compromised in GBPchr3$^{-/-}$ cells compared to wild-type (Fig. 6D), as observed by lower LC3-II conversion. During

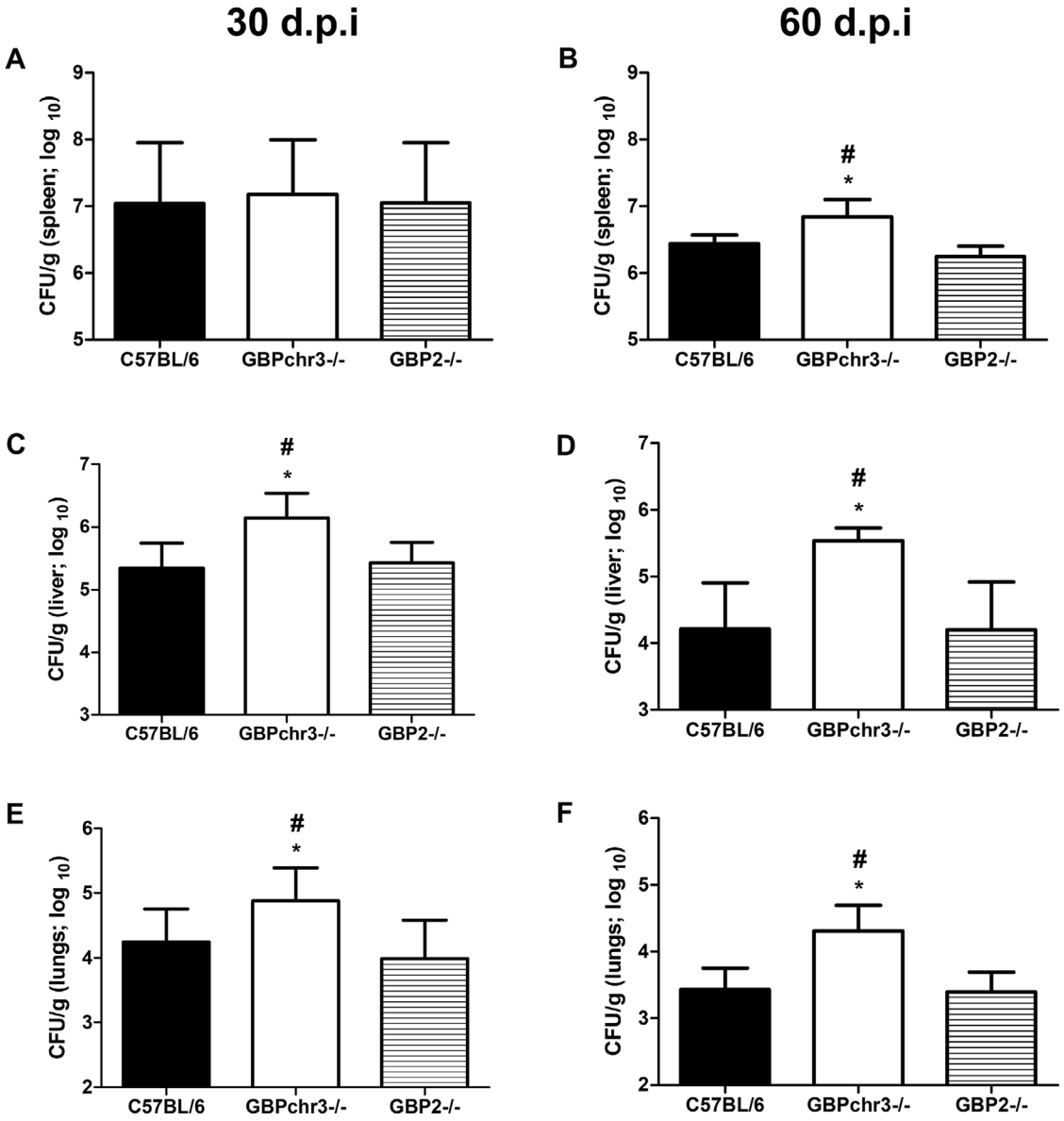

FIGURE 2 **Lack of guanylate binding proteins (GBPs) from chromosome 3 (GBPchr3) increases susceptibility to *Mycobacterium bovis* BCG infection.** Mice were infected i.v. with 1×10^6 CFU of *M. bovis* BCG. The spleens (**A, B**), livers (**C, D**) and lungs (**E, F**) from 30 or 60 d infected mice were collected, homogenized, and plated for CFU counting. Graphs are representative of three independent experiments performed. $^*P < 0.05$ compared to C57BL/6; $\#P < 0.05$ compared to GBP2$^{-/-}$

maturation, the autophagosome inner membrane is degraded by lysosomal enzymes, a process known as autophagic flux.[32] An interruption in autophagosome-lysosome fusion also leads to accumulation of LC3-II. Thus, the increase in LC3-II levels detected in *M. bovis* BCG-infected cells could indicate either an active induction of autophagy or an inhibition of autophagic flux. To distinguish both process, cells were stimulated in presence of Bafilomycin A1 (Baf), an endosomal acidification inhibitor that blocks autophagic flux. Upon Baf treatment, both wild-type and GBPchr3$^{-/-}$ *M. bovis* BCG-infected cells presented higher LC3-II conversion compared to nontreated cells (Supporting Information Fig. S5B). However, evaluating specifically Baf-treated cells, LC3-II levels in infected cells were slightly lower than in noninfected cells, indicating that *M. bovis* BCG is able to partially block the autophagic flux. Besides that, it is noteworthy that there are lower LC3-II levels in infected/Baf-treated GBPchr3$^{-/-}$ cells compared to their wild-type counterparts, in a similar pattern to the observation in Figure 6D, indicating that lack of GBPs does not alter autophagic flux but instead influences autophagy induction. Overall, these compromised immunologic components (cytokines, NO, and autophagy) correlated with deficient intracellular killing of *M. bovis* BCG in GBPchr3$^{-/-}$ macrophages (Fig. 6E). In summary, these results suggest that GBPchr3 are necessary for myeloid cells activation, influencing cell-intrinsic immunity and the establishment of efficient immune response to control mycobacterial infection.

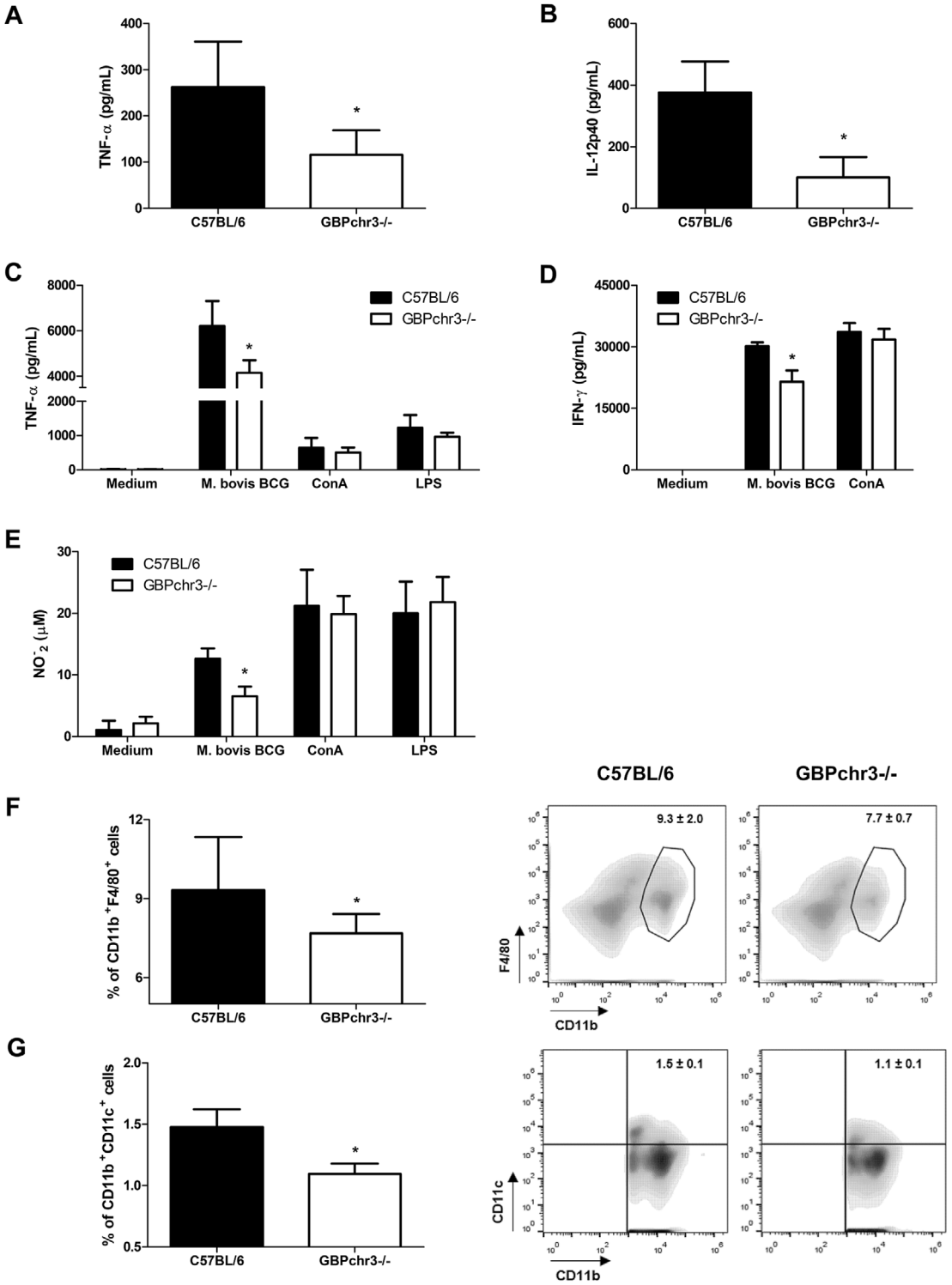

FIGURE 3 **Deficiency of guanylate binding proteins (GBPs) from chromosome 3 (GBPchr3) alters cytokine production and myeloid cells presence in spleen during early *Mycobacterium bovis* BCG infection.** (**A, B**) Bronchoalveolar lavage from infected mice was collected and the levels of TNF-α and IL-12p40 were evaluated by ELISA. (**C, D**) Spleen cells were cultivated in the presence of the mentioned stimuli for evaluation of TNF-α and IFN-γ recall responses. (**E**) NO production was evaluated by the Griess method in supernatants of 72 h stimulated cells.

(Continued on next page)

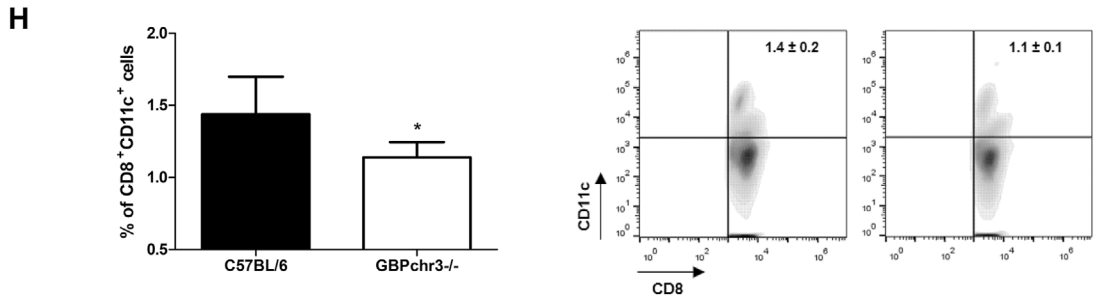

FIGURE 3 (Continued) (**F, G, H**) Spleen cells were stained ex vivo and flow cytometry was performed to measure the frequency of macrophages ($CD11b^+F4/80^+$) or subpopulations of dendritic cells ($CD11b^+CD11c^+$ or $CD8^+CD11c^+$). All these experiments were conducted in 30 d infected mice. Graphs are representative of at least two performed experiments. $^*P < 0.05$ compared to C57BL/6

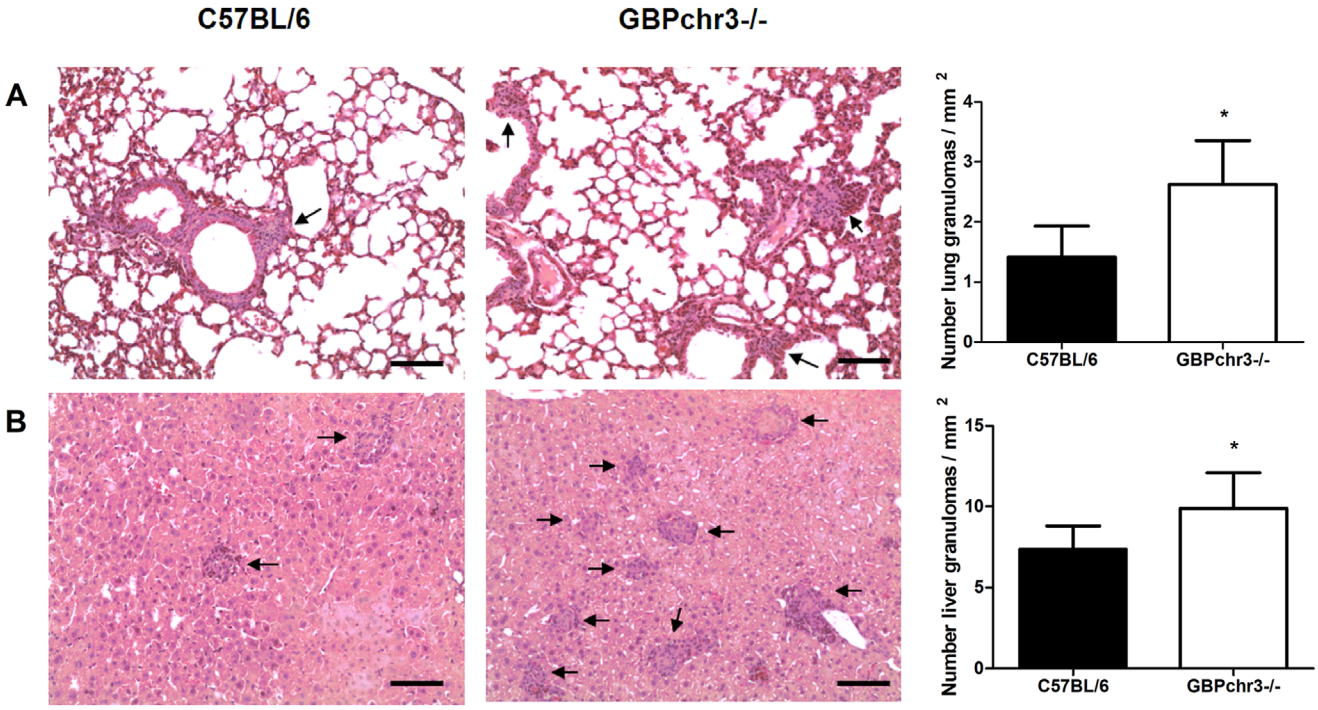

FIGURE 4 **Increased granuloma burden in lungs and liver during *Mycobacterium bovis* BCG early infection in guanylate binding proteins (GBPs) from chromosome 3 (GBPchr3)-deficient mice.** Fragments of lungs and liver from *M. bovis* BCG infected mice were collected after 30 d.p.i and embedded in paraffin. The resulting slides were evaluated for the number of granulomas in the parenchyma of (**A**) lung and (**B**) liver, and normalized by the covered area (in square millimeters). Representative images of each group are shown. The arrows indicate examples of granulomas. H&E. Scale bars: 80 μm. Average of two experiments performed. $^*P < 0.05$ compared to C57BL/6

4 | DISCUSSION

In this study, we addressed the influence of the cluster of GBPchr3 (namely GBP1, 2, 3, 5 and 7) in host immunity against mycobacterial infection to further elucidate the relationship between myeloid cell-intrinsic immunity and the triggering of an efficient immune response. We found that GBPchr3 have enhanced expression during early infection with *M. bovis* BCG. In lungs, these proteins follow the kinetics of IFN-γ expression and they are also important for regulating the expression of autophagy-related genes *LC3B*, *ULK1*, and *ATG5*. In vivo, the cluster of GBPchr3 is important to control bacterial burden, affecting the production of proinflammatory cytokines, and the activation and the influx of myeloid cells in spleens. These data correlate with reduced DCs activation and decreased microbicidal capacity of macrophages in vitro due to absence of GBPchr3. Moreover, our findings demonstrate a dispensable role for GBP2 to control bacterial burden in vivo.

Despite intense efforts, TB and other mycobacterial-promoted diseases are still a major public health problem.[10,33] Inefficient treatments and emerging bacterial resistance to antibiotics generate a need for novel strategies, whose development requires an improved understanding of host-pathogen relationship. In this regard, the study of *M. bovis* BCG infection is important once this vaccine retain great part of the virulence factors carried by pathogenic mycobacteria, being able even to promote disseminated infection in immunocompromised patients.[23,34] The expression of the cluster of GBPchr3 was highly induced in lungs of infected mice, mainly during early infection. It is

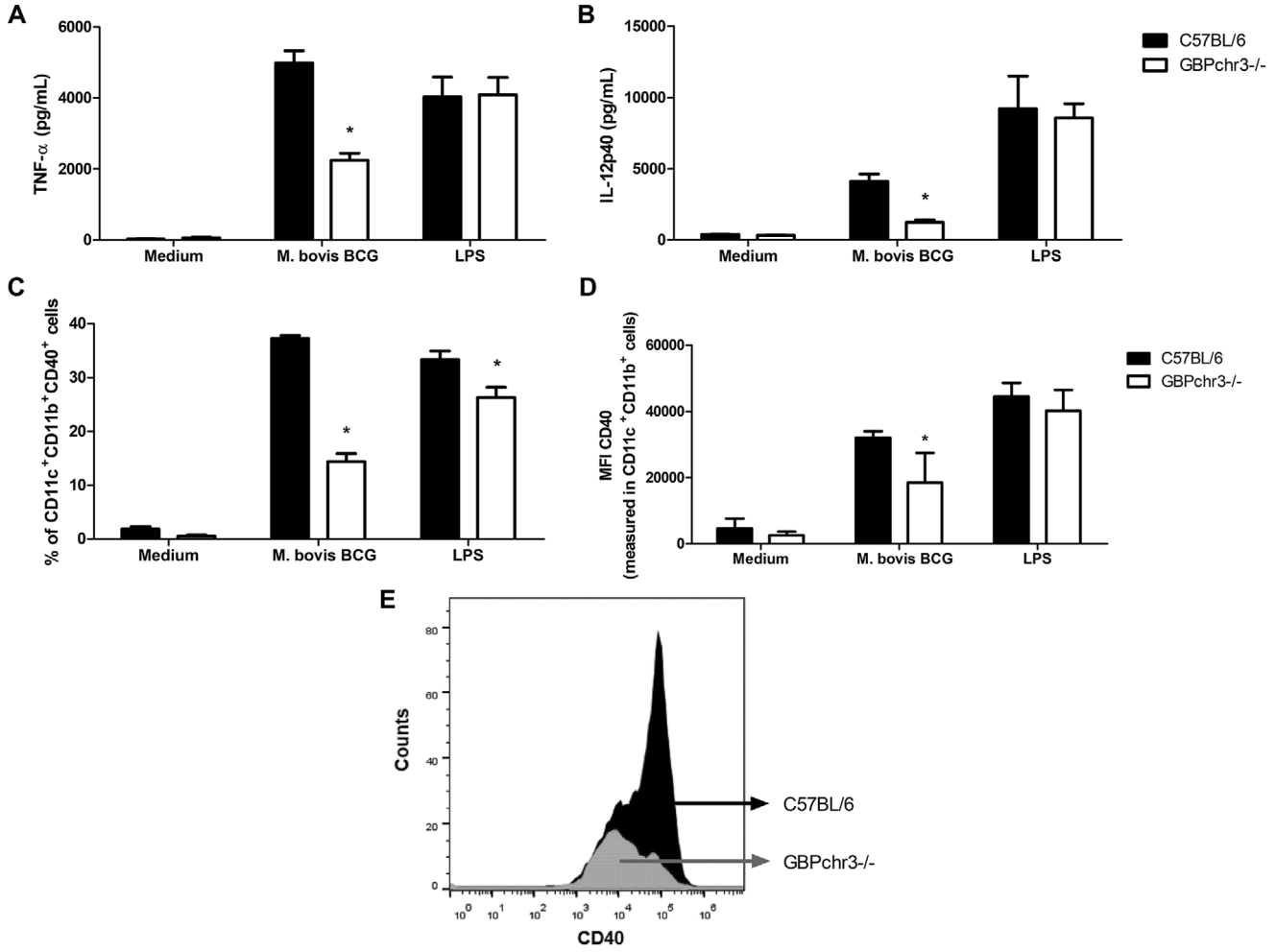

FIGURE 5 **Absence of guanylate binding proteins (GBPs) from chromosome 3 (GBPchr3) hampers dendritic cells activation in response to *Mycobacterium bovis* BCG.** Bone marrow-derived dendritic cells were derived from C57BL/6 or GBPchr3$^{-/-}$ mice and stimulated during 24 h with *M. bovis* BCG (multiplicity of infection [MOI] 5:1) or LPS (100 ng/mL) for evaluation of TNF-α (**A**) and IL-12p40 (**B**) production by ELISA or CD40 expression by flow cytometry (**C, D**). (**E**) An illustrative plot of the frequency and intensity of CD40 expression is showed. Graphs are representative of at least two performed experiments. *$P < 0.05$ compared to C57BL/6

interesting to note that *GBP5* was the most induced, followed by *GBP2*, *GBP3*, and *GBP7*. This result is in line with the finding that GBP5 is a great candidate for TB signature biomarker, as it differentiates this infection from other pulmonary diseases due to its high expression in whole blood sample of patients.[35] On the other hand, we observed a slight up-regulation of GBP1, compared to the other GBPchr3. Indeed, in vivo expression of GBP1 is a matter of debate as the level of mRNA may not be indicative of protein translation.[2,36] At later time point, all GBPs analyzed presented similar up-regulation levels, significantly diminished compared to early infection period. This pattern correlated with the expression levels observed for *IFN-γ* and *IFN-β*, suggesting their roles as the major inducers of GBPs. Additionally, absence of GBPchr3 reduced the expression of *LC3B*, *ULK1*, and *ATG5*, molecules important for autophagy. LC3B is a crucial autophagic marker due to its association with autophagosome membrane.[32] ULK1 is a core protein of the ULK1 complex, an autophagy-specific complex that comes into play upon autophagy induction.[30] ATG5 is involved in the elongation of isolation membrane during autophagosome formation, being relevant to limit *M. tuberculosis* growth in vivo.[37] The expression pattern found in lungs in response to early infection suggests that both GBPs and autophagy pathways are aligned.

The role of GBPs during mycobacterial infections was first addressed by Kim and colleagues.[28] They showed that mice deficient in GBP1 present increased bacterial burden becoming moribund about 10 to 14 wk postinfection with *M. bovis* BCG Phipps strain, the most virulent among BCG vaccine strains. Herein, by using a moderate virulent strain (Moreau), we showed that GBPchr3 are important to control the bacterial burden, in line with the previous finding. The lack of the entire GBPchr3 locus also resulted in increased pathology, represented by higher number of granulomas in liver and lungs compared to wild-type mice. However, the level of *GBP1* expression in our study was the lowest compared to other GBPs contained in mouse chromosome 3. Additionally, absence of the entire locus of GBPchr3 resulted in lower proinflammatory cytokines level in both bronchoalveolar lavage and spleen cells recall response that reflects systemic hampering of myeloid cell activation, especially CD11b+ DCs. This subpopulation

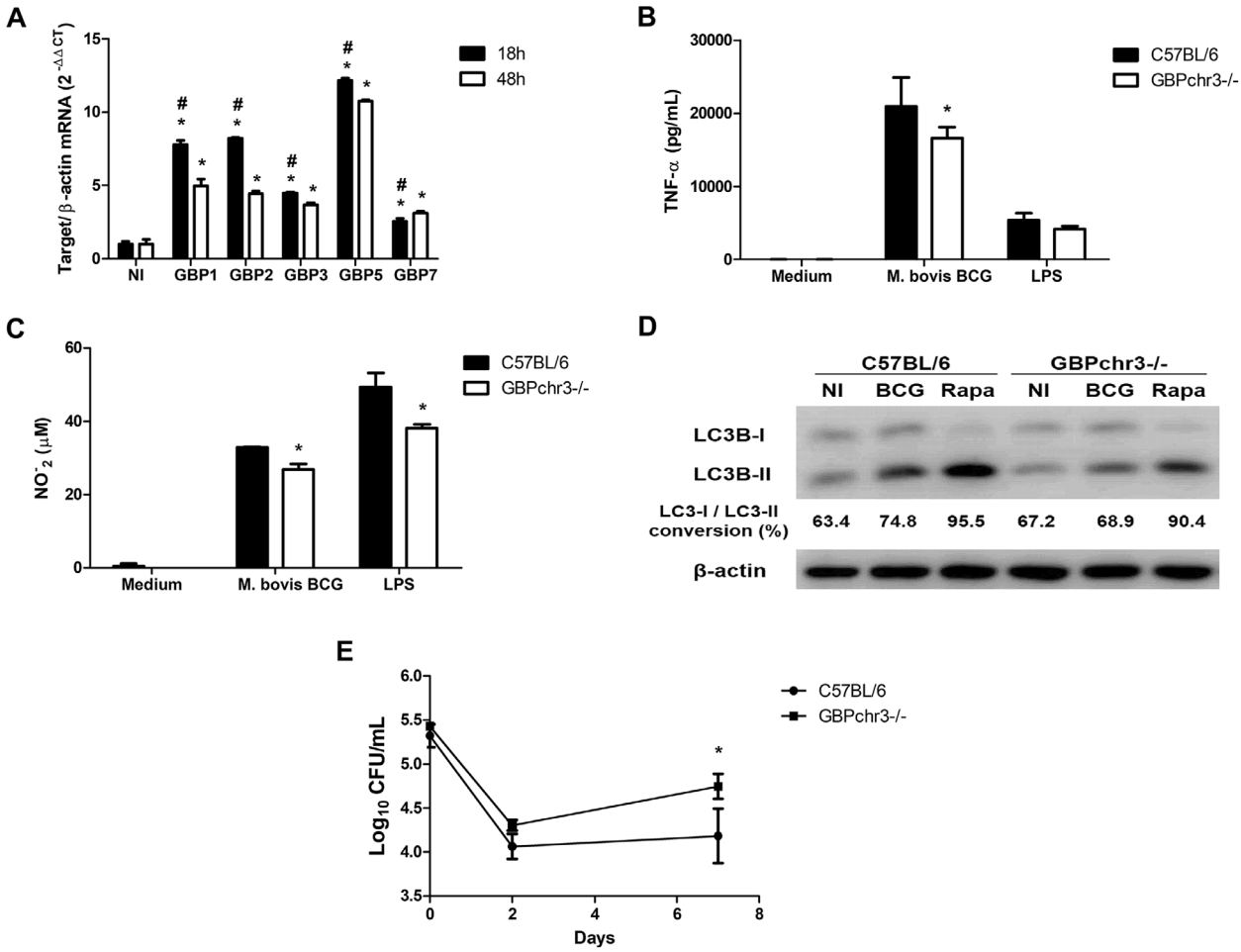

FIGURE 6 **Deficiency of guanylate binding proteins (GBPs) from chromosome 3 (GBPchr3) decreases macrophages antimicrobial function in response to *Mycobacterium bovis* BCG.** (**A**) Bone marrow-derived macrophages (BMDMs) were derived from C57BL/6 mice and stimulated with *M. bovis* BCG (multiplicity of infection [MOI] 5:1) for evaluation of GBPs expression by qPCR at selected time points. The gene expression was evaluated by qPCR relative to *β-actin* RNA. $^{*}P < 0.05$ compared to NI; $\#P < 0.05$ compared to 48 h. (**B**) Wild-type or GBPchr3$^{-/-}$ BMDM were stimulated for 24 h with *M. bovis* BCG (MOI 5:1) or LPS (100 ng/mL) and TNF-α production was evaluated. (**C**) BMDMs were incubated overnight with recombinant murine IFN-γ (10 ng/mL) and stimulated for 24 h with *M. bovis* BCG or LPS as mentioned earlier. The NO production was evaluated by the Griess method. (**D**) The analysis of LC3 conversion by Western blot was performed after 4 h stimulation with *M. bovis* BCG (MOI 50:1) or rapamycin (15 μg/mL). β-actin was used as loading control. Each band was quantified by densitometry. The value of LC3-I/LC3-II conversion is showed. (**E**) The intracellular bacterial burden in macrophages was evaluated after up to 7 d postinfection. Graphs are representative of at least two performed experiments. NI: noninfected and $^{*}P < 0.05$ compared to C57BL/6

of cDCs is more efficient in direct CD4+ T cell responses and is an important source of proinflammatory cytokines.[31] Moreover, the presence of macrophages and both subpopulations of cDCs in spleen of GBPchr3$^{-/-}$ mice was reduced compared to their wild-type counterparts. These alterations in the immune response were more pronounced during early infection period. By contrast, the population of CD4+ T cells was higher in knockout mice throughout the infection. This fact may be result of a compensatory effect balancing the reduced and/or insufficiently activated myeloid cell populations. Additional experiments are needed to investigate further this phenomenon. The importance of the cluster of GBPchr3 has been addressed in other infections. GBPchr3 are required to disrupt *Toxoplasma gondii* PCVs and to control parasite replication in mice.[38] Similarly, GBPchr3 are required to lyse *Salmonella*-containing vacuoles and *Francisella novicida* cytosolic bacterium, leading to activation of canonical and noncanonic inflammasomes and limiting both pathogens growth.[39,40] However, these reports did not find alterations concerning cell migration or autophagy, suggesting that these features may be related to the disease studied.

At the onset of mycobacterial infection, macrophages and DCs are the host immune cells frontline against the bacilli. Both cells instruct the establishment of an efficient immune response through the production of proinflammatory molecules while trying to limit pathogen growth.[41] The role of GBPs on DCs activation seems to be less studied and there are few reports focusing on this theme.[42,43] The lack of GBPchr3 drastically reduced the production of the proinflammatory cytokines TNF-α and IL-12, associated with diminished expression of CD40, in response to *M. bovis* BCG. Indeed, a reduced expression

of this costimulatory molecule was also found in unstimulated cells, although it was not statistically significant. This could suggest that GBPchr3 may also influence DCs differentiation and autonomous activation independent of the antigen. This data is in agreement with what has been recently shown concerning murine GBP2 regulation of DCs maturation.[43] Regarding the role of GBPs in macrophages, in this study, we show that *M. bovis* BCG was able to induce GBPchr3 expression in these cells. GBP5 was the highest expressed GBP when compared to the others analyzed. Concerning mycobacterial infection in macrophages, GBP1 and GBP7 were reported to be important for autophagy induction, with an additional role for GBP7 by recruiting NADPH oxidase subunits. The absence of these individual GBPs correlated with increased bacterial burden in 48 h short spanning killing assay.[28] Here, we demonstrate that the absence of the entire locus of GBPchr3 reduced BCG-induced autophagy and NO production, associated with increased bacterial burden in 7 d in vitro assay. The increased bacterial burden found in vivo may reflect these dampened antimicrobial mechanisms observed in GBPchr3-deficient animals. Furthermore, infected GBPchr3$^{-/-}$ macrophages showed a slight reduction in TNF-α production, in line with the reduced TNF-α MFI found during early in vivo infection. Altogether, these results confirm GBPchr3 as important molecules necessary for myeloid cells to accomplish their role in immune response against mycobacterial infection.

Mycobacterial infections, especially TB and opportunistic infections in immunocompromised patients, remain a global concern. In summary, this study highlights the relevance of GBPchr3 during early *M. bovis* BCG infection. These GBPs are highly up-regulated in lungs of infected host and act influencing myeloid cell function, particularly DC activation and the antimicrobial capacity of macrophages that culminates in control of bacterial burden. This work expands the knowledge of GBPs role during mycobacterial infection by showing their effect in proinflammatory cytokines production and places them as relevant regulators of an efficient immune response. Indeed, there is increasing amount of information concerning GBPs up-regulation during human mycobacterial infections.[35,44] Their definitive roles during human infections remain to be demonstrated. The links between cell-intrinsic immunity and the overall establishment immune response open venues to be explored for improved therapy and preventive medicine.

ACKNOWLEDGMENTS

This work was supported by grants from Conselho Nacional de Desenvolvimento Cientifico e Tecnologico (CNPq) grant #465229/2014-0, 401209/2020-2 and 302660/2015-1 (to S.C.O.) and 421867/2018-3 (to A. J-K) and Fundação de Amparo à Pesquisa do Estado de São Paulo (FAPESP) grant #2017/24832-6 (to S.C.O.) and Coordenação de Aperfeiçoamento de Pessoal de Nível Superior (CAPES) grant #88887.506611/202-00 and National Institutes of Health R01 AI116453 (to S.C.O.). F.M. was supported by grants from CNPq #150044/2017-8 and CAPES #88887-364940/2019-00.

AUTHORSHIP

F.V.M. and S.C.O. conceptualized this study; F.V.M., J.S.F., A.C.V.S.C.A, L.T.S.D., M.T.R.G., D.P.R., and A.P.J.-K. were responsible for the investigation; F.V.M., J.S.F., and M.T.R.G. were in charge of data curation and formal analysis; and F.V.M. and S.C.O. wrote the original draft and the final manuscript.

DISCLOSURES

The authors declare no conflicts of interest.

ORCID

Fabio V. Marinho https://orcid.org/0000-0001-6885-3438
Sergio C. Oliveira https://orcid.org/0000-0003-4062-5577

REFERENCES

1. Santos JC, Broz P. Sensing of invading pathogens by GBPs: at the crossroads between cell-autonomous and innate immunity. *J Leukoc Biol*. 2018;104:729-735.
2. Degrandi D, Konermann C, Beuter-Gunia C, et al. Extensive characterization of IFN-induced GTPases mGBP1 to mGBP10 involved in host defense. *J Immunol*. 2007;179:7729-7740.
3. Olszewski MA, Gray J, Vestal DJ. In silico genomic analysis of the human and murine guanylate-binding protein (GBP) gene clusters. *J Interferon Cytokine Res*. 2006;26:328-352.
4. Kresse A, Konermann C, Degrandi D, et al. Analyses of murine GBP homology clusters based on in silico, in vitro and in vivo studies. *BMC Genomics*. 2008;9:158.
5. Kravets E, Degrandi D, Ma Q, et al. Guanylate binding proteins directly attack *Toxoplasma gondii* via supramolecular complexes. *Elife*. 2016;5:e11479.
6. Ngo CC, Man SM. Mechanisms and functions of guanylate-binding proteins and related interferon-inducible GTPases: roles in intracellular lysis of pathogens. *Cell Microbiol*. 2017;19.
7. Praefcke GJK. Regulation of innate immune functions by guanylate-binding proteins. *Int J Med Microbiol*. 2018;308:237-245.
8. Finethy R, Jorgensen I, Haldar AK, et al. Guanylate binding proteins enable rapid activation of canonical and noncanonical inflammasomes in Chlamydia-infected macrophages. *Infect Immun*. 2015;83:4740-4749.
9. Gomes MTR, Cerqueira DM, Guimaraes ES, Campos PC, Oliveira SC. Guanylate-binding proteins at the crossroad of noncanonical inflammasome activation during bacterial infections. *J Leukoc Biol*. 2019;106:553-562.
10. World Health Organization (2019) Global Tuberculosis Report.
11. Zhang L, Ru HW, Chen FZ, et al. Variable virulence and efficacy of BCG vaccine strains in mice and correlation with genome polymorphisms. *Mol Ther*. 2016;24:398-405.
12. Awuh JA, Flo TH. Molecular basis of mycobacterial survival in macrophages. *Cell Mol Life Sci*. 2017;74:1625-1648.
13. Kuehnel MP, Goethe R, Habermann A, et al. Characterization of the intracellular survival of *Mycobacterium avium* ssp. paratuberculosis: phagosomal pH and fusogenicity in J774 macrophages compared with other mycobacteria. *Cell Microbiol*. 2001;3:551-566.
14. Rumsey J, Valentine JF, Naser SA. Inhibition of phagosome maturation and survival of *Mycobacterium avium* subspecies paratuberculosis in polymorphonuclear leukocytes from Crohn's disease patients. *Med Sci Monit*. 2006;12:BR130-9.

15. Kang PB, Azad AK, Torrelles JB, et al. The human macrophage mannose receptor directs *Mycobacterium tuberculosis* lipoarabinomannan-mediated phagosome biogenesis. *J Exp Med*. 2005;202:987-999.
16. Bourigault ML, Segueni N, Rose S, et al. Relative contribution of IL-1alpha, IL-1beta and TNF to the host response to *Mycobacterium tuberculosis* and attenuated *M. bovis* BCG. *Immun Inflamm Dis*. 2013;1:47-62.
17. Flynn JL, Chan J, Triebold KJ, Dalton DK, Stewart TA, Bloom BR. An essential role for interferon gamma in resistance to *Mycobacterium tuberculosis* infection. *J Exp Med*. 1993;178:2249-2254.
18. Tuerlinckx D, Vermylen C, Brichard B, Ninane J, Cornu G. Disseminated *Mycobacterium avium* infection in a child with decreased tumour necrosis factor production. *Eur J Pediatr*. 1997;156:204-206.
19. Ehlers S, Richter E. Gamma interferon is essential for clearing *Mycobacterium genavense* infection. *Infect Immun*. 2000;68:3720-3723.
20. Chan J, Xing Y, Magliozzo RS, Bloom BR. Killing of virulent *Mycobacterium tuberculosis* by reactive nitrogen intermediates produced by activated murine macrophages. *J Exp Med*. 1992;175:1111-1122.
21. Via LE, Fratti RA, McFalone M, Pagan-Ramos E, Deretic D, Deretic V. Effects of cytokines on mycobacterial phagosome maturation. *J Cell Sci*. 1998;111(Pt 7):897-905.
22. Harris J, Hope JC, Keane J. Tumor necrosis factor blockers influence macrophage responses to *Mycobacterium tuberculosis*. *J Infect Dis*. 2008;198:1842-1850.
23. Pourakbari B, Hosseinpour Sadeghi R, Mahmoudi S, Parvaneh N, Keshavarz Valian S, Mamishi S. Evaluation of interleukin-12 receptor beta1 and interferon gamma receptor 1 deficiency in patients with disseminated BCG infection. *Allergol Immunopathol (Madr)*. 2019;47:38-42.
24. MacMicking JD, Taylor GA, McKinney JD. Immune control of tuberculosis by IFN-gamma-inducible LRG-47. *Science*. 2003;302:654-659.
25. Singh SB, Davis AS, Taylor GA, Deretic V. Human IRGM induces autophagy to eliminate intracellular mycobacteria. *Science*. 2006;313:1438-1441.
26. Feng CG, Collazo-Custodio CM, Eckhaus M, et al. Mice deficient in LRG-47 display increased susceptibility to mycobacterial infection associated with the induction of lymphopenia. *J Immunol*. 2004;172:1163-1168.
27. Boehm U, Guethlein L, Klamp T, et al. Two families of GTPases dominate the complex cellular response to IFN-gamma. *J Immunol*. 1998;161:6715-6723.
28. Kim BH, Shenoy AR, Kumar P, Das R, Tiwari S, MacMicking JD. A family of IFN-gamma-inducible 65-kD GTPases protects against bacterial infection. *Science*. 2011;332:717-721.
29. Deretic V, Levine B. Autophagy, immunity, and microbial adaptations. *Cell Host Microbe*. 2009;5:527-549.
30. Zachari M, Ganley IG. The mammalian ULK1 complex and autophagy initiation. *Essays Biochem*. 2017;61:585-596.
31. Merad M, Sathe P, Helft J, Miller J, Mortha A. The dendritic cell lineage: ontogeny and function of dendritic cells and their subsets in the steady state and the inflamed setting. *Annu Rev Immunol*. 2013;31:563-604.
32. Klionsky DJ, Abdelmohsen K, Abe A, Abedin MJ, Abeliovich H, et al. Guidelines for the use and interpretation of assays for monitoring autophagy (3rd edition). *Autophagy*. 2016;12:1-222.
33. Brode SK, Daley CL, Marras TK. The epidemiologic relationship between tuberculosis and non-tuberculous mycobacterial disease: a systematic review. *Int J Tuberc Lung Dis*. 2014;18:1370-1377.
34. World Health Organization (2018) BCG vaccine: WHO position paper, February 2018—recommendations. *Vaccine* 36, 3408-3410.
35. Laux da Costa L, Delcroix M, Dalla Costa ER, et al. A real-time PCR signature to discriminate between tuberculosis and other pulmonary diseases. *Tuberculosis (Edinb)*. 2015;95:421-425.
36. Clough B, Finethy R, Khan RT, et al. C57BL/6 and 129 inbred mouse strains differ in Gbp2 and Gbp2b expression in response to inflammatory stimuli in vivo. *Wellcome Open Res*. 2019;4:124.
37. Castillo EF, Dekonenko A, Arko-Mensah J, et al. Autophagy protects against active tuberculosis by suppressing bacterial burden and inflammation. *Proc Natl Acad Sci U S A*. 2012;109:E3168-76.
38. Yamamoto M, Okuyama M, Ma JS, et al. A cluster of interferon-gamma-inducible p65 GTPases plays a critical role in host defense against *Toxoplasma gondii*. *Immunity*. 2012;37:302-313.
39. Meunier E, Dick MS, Dreier RF, et al. Caspase-11 activation requires lysis of pathogen-containing vacuoles by IFN-induced GTPases. *Nature*. 2014;509:366-370.
40. Wallet P, Benaoudia S, Mosnier A, et al. IFN-gamma extends the immune functions of guanylate binding proteins to inflammasome-independent antibacterial activities during *Francisella novicida* infection. *PLoS Pathog*. 2017;13:e1006630.
41. Korbel DS, Schneider BE, Schaible UE. Innate immunity in tuberculosis: myths and truth. *Microbes Infect*. 2008;10:995-1004.
42. Fiegl D, Kagebein D, Liebler-Tenorio EM, et al. Amphisomal route of MHC class I cross-presentation in bacteria-infected dendritic cells. *J Immunol*. 2013;190:2791-2806.
43. Zhang S, Feng T, Ning Y, Zhang X, Qi C. [Guanylate-binding protein 2 regulates the maturation of mouse dendritic cells induced by beta-glucan]. *Xi Bao Yu Fen Zi Mian Yi Xue Za Zhi*. 2017;33:1153-1159.
44. Teles RMB, Lu J, Tio-Coma M, et al. Identification of a systemic interferon-gamma inducible antimicrobial gene signature in leprosy patients undergoing reversal reaction. *PLoS Negl Trop Dis*. 2019;13:e0007764.

SUPPORTING INFORMATION

Additional information may be found online in the Supporting Information section at the end of the article.

How to cite this article: Marinho FV, Fahel JS, de Araujo ACVSC, et al. Guanylate binding proteins contained in the murine chromosome 3 are important to control mycobacterial infection. *J Leukoc Biol*. 2020;108:1279–1291. https://doi.org/10.1002/JLB.4MA0620-526RR